Biosensors and Bioelectronics 26 (2010) 43–49

Contents lists available at ScienceDirect

Biosensors and Bioelectronics

journal homepage: www.elsevier.com/locate/bios

Enzyme functionalized nanoparticles for electrochemical biosensors: A comparative study with applications for the detection of bisphenol A

Ramiz S.J. Alkasir[a], Mallikarjunarao Ganesana[a], Yu-Ho Won[b], Lia Stanciu[b], Silvana Andreescu[a,*]

[a] Department of Chemistry and Biomolecular Science, Clarkson University, 8 Clarkson Ave., Potsdam, NY 13699-5810, United States
[b] School of Materials Engineering and Birck Nanotechnology Center, Purdue University, West Lafayette, IN 47907, United States

ARTICLE INFO

Article history:
Received 13 February 2010
Received in revised form 17 April 2010
Accepted 2 May 2010
Available online 10 May 2010

Keywords:
Tyrosinase
Bisphenol A
Magnetic
Iron oxide
Nickel
Gold
Nanoparticles
Screen-printed electrodes

ABSTRACT

We developed electrochemical biosensors based on enzyme functionalized nanoparticles of different compositions for the detection of bisphenol A. We utilized for the first time magnetic nickel nanoparticles as an enzyme immobilization platform and electrode material to construct screen-printing enzyme biosensors for bisphenol A. We compared the analytical performance of these sensors with those based on iron oxide (Fe_3O_4) and gold nanoparticles. The proposed biosensor format exhibited fast and sensitive amperometric responses to bisphenol A with a response time of less then 30 s. Among the three configurations, nickel provided comparable or better characteristics in terms of detection limit and sensitivity than Fe_3O_4 and gold nanoparticles. The biosensors were characterized by good reproducibility, stability of more than 100 assays (residual activity for nickel was 98%) and a wide linear range which spanned from 9.1×10^{-7} to 4.8×10^{-5} M for nickel, 2.2×10^{-8} to 4.0×10^{-5} M for Fe_3O_4 and 4.2×10^{-8} to 3.6×10^{-5} M for gold. The highest sensitivity was obtained with nickel. The detection limits for the three types of biosensors were: 7.1×10^{-9}, 8.3×10^{-9} and 1×10^{-8} M for nickel, Fe_3O_4 and gold nanoparticles in that order, respectively. These results demonstrate that nickel nanoparticles can be successfully used in the construction of electrochemical enzyme sensors for the detection of phenolic compounds.

1. Introduction

In recent years, several types of magnetic nanoparticles and composites of these materials have been used to construct electrochemical enzyme based sensors. These materials have been traditionally used as magnetic carriers in bio-separations (Park et al., 2007) and detection (Rossi et al., 2004). In the biosensors field they have provided magnetic control of electrochemical processes (Katz and Willner, 2002; Wang et al., 2005) and ensured transport of immobilized biomolecules at electrode surfaces (Loaiza et al., 2007), thus creating possibilities for regeneration and reuse. Magnetic beads with immobilized glucose oxidase have been magnetically retained within the flow line of a flow injection system designed to detect glucose using amperometric methods (Nomura et al., 2004). Combining magnetic manipulation with bio-immobilization, separation and detection have provided unique capabilities and improved performance of biosensing devices (Stanciu et al., 2009). Enzymatic sensors based on various bio-functionalized magnetic platforms (Chen and Liao, 2002; Rossi et al., 2004) have been designed with high enzyme loading and possibilities for controlling the localization of the enzyme–nanoparticles bio-conjugate through the use of a magnet placed underneath the electrode (Istarnboulie et al., 2007; Liu et al., 2005). Examples include sensors based on tyrosinase for the detection of phenol (Liu et al., 2005; Wang et al., 2008), glucose oxidase for glucose (Lu and Chen, 2006) and acetylcholinesterase for organophosphate pesticides (Istarnboulie et al., 2007; Won et al., 2010).

Due to their simple preparation, easy functionalization and paramagnetic properties, iron oxide-based nanoparticles (Fe_2O_3, Fe_3O_4 and core–shell particles) have been the most widely used in these applications. As an alternative, magnetic nickel nanoparticles and nanowires can also be used to control electrochemical processes and create magneto-switchable devices (Wang et al., 2005, 2006). However, in spite of their interesting electrocatalytic and magnetic properties, biosensing applications of nickel nanostructures are scarcely reported. In previous works, nickel nanowires have promoted electrocatalytic oxidation of glucose in the absence of enzyme in alkaline medium (Lu et al., 2009). Nickel nanoparticles electrodeposited onto a glassy carbon electrode have been used for the immobilization of hemoglobin (Salimi et al., 2006) and for the electrocatalysis of glucose oxidase for glucose detection (Salimi et al., 2007). We report herein the use of enzyme functionalized nickel nanoparticles to fabricate screen-printed electrodes for the detection of bisphenol A. We compare the analytical performance of these sensors with those based on iron oxide nanoparticles and

* Corresponding author. Tel.: +1 315 268 2394; fax: +1 315 268 6610.
E-mail address: eandrees@clarkson.edu (S. Andreescu).

0956-5663/$ – see front matter © 2010 Elsevier B.V. All rights reserved.
doi:10.1016/j.bios.2010.05.001

with those based on the more traditionally used gold nanoparticles (Liu et al., 2003; Mena et al., 2005; Sanz et al., 2005; Tu et al., 2009).

Bisphenol A (BPA) is an industrially important chemical used in the production of polycarbonate plastics, epoxy resins, dental sealants, and food packaging. Recently, it has received considerable attention due to its endocrine disrupting activity and possible toxic environmental and health impacts (Ballesteros-Gomez et al., 2009; Kang et al., 2006; Le et al., 2008). BPA levels in the low μg/L range could be found in clinical, food and water samples (Dekant and Voelkel, 2008; Volkel et al., 2008). Traditional detection methods for BPA include chromatographic techniques coupled with mass spectrometry, capillary electrophoresis and solid phase microextraction (Chang et al., 2005; Nerin et al., 2002), which are time consuming, cannot be performed on-site and require sample pretreatment steps. Electrochemical sensors can provide rapid and on-site detection of BPA. Several tyrosinase biosensors based on carbon paste, glassy carbon and boron doped diamond electrodes have been reported for this purpose (Andreescu and Sadik, 2004; Mita et al., 2007; Notsu et al., 2002). Most of these sensors have been used for the detection of simple phenolic compounds, mainly phenol and catechol, with the enzyme immobilized on traditional carbon materials. More recently, tyrosinase was immobilized on metal and metal oxide nanoparticles such as Au nanoparticles (Sanz et al., 2005), titanium oxide (Chen et al., 2001), zinc oxide (Li et al., 2006), iron oxide (Wang et al., 2008) and polypyrrole–gold nanocomposites (Njagi and Andreescu, 2007). In this work, we utilize for the first time nickel nanoparticles as an enzyme immobilization platform and electrode material to construct a BPA screen-printing sensor with magnetically reloadable surface. The proposed biosensor was developed on a screen-printing electrode platform, which is the preferred format for the development of inexpensive detection systems and portable instrumentation for food and environmental analysis (Avramescu et al., 2002). We demonstrate that nickel can be successfully used as electrode material for electrochemical enzyme biosensors, providing comparable or better characteristics than Fe_3O_4 and Au nanoparticles. The biosensors described in this work show great promise for the ultrasensitive, rapid and cost-effective analysis of BPA in aqueous solutions.

2. Experimental

2.1. Reagents and stock solutions

Tyrosinase (EC.1.14.18.1, from *Mushroom*, 5370 U mg^{-1} lyophilized powder), bisphenol A (99+%), tyrosine, catechol, phenol, glucose, ascorbic acid, uric acid and gold (III) chloride trihydrate $HAuCl_4{\cdot}3H_2O$ (≥49.0% Au basis) were purchased from Sigma (St. Louis, MO, USA). Glutaraldehyde solution (25%) was purchased from Acros (NJ, USA). Fe_3O_4 nanoparticles with a diameter of 10 nm, conjugated with amino functional groups were prepared as described in the literature (Rossi et al., 2004). Well dispersed spherical nickel nanoparticles of uniform size with a diameter of 30 nm were prepared using established procedure via the polyol process (Fievet and Figlarz, 1989), starting from nickel carbonate (Sheperd Chem., USA), $PtCl_4$ (Umicore, Germany) as a catalyst and the polyol-propyleneglycol (Alfa Aesar, USA) as solvent/reducing agent. Complete physicochemical characterization (size, charge, morphology and particle size distribution) of these nanoparticles was described in detail in a recent work (Ispas et al., 2009). Nickel nanoparticles were amino-functionalized as described previously (Huang et al., 2003), using the same procedure as that for magnetite. Potassium phosphate monobasic was supplied from Fisher Scientific. Sodium phosphate (dibasic, anhydrous) was purchased from J.T. Baker (Phillipsburg, NJ, USA). A solution of 2×10^{-2} M potassium hexacyanoferrate (III) prepared in 0.2 M potassium chloride was used in cyclic voltammetric experiments to determine the electrochemical surface area of the electrodes. A stock solution of 1×10^{-2} M BPA was prepared in methanol and stored at 4 °C for not more than 3 weeks. Working solutions of BPA were prepared in phosphate buffer (PBS) at pH 6.5 daily. A stock solution of 1×10^{-2} M $HAuCl_4$ was prepared in Milli-Q water. All reagents were used without further purification and all solutions were prepared with distilled, deionized water (Millipore, Direct-Q system) with a resistivity of 18.2 MΩ.

2.2. Apparatus and electrodes

Cyclic voltammetry (CV) and amperometric experiments were performed with an Epsilon potentiostat (Bioanalytical Systems Inc., West Lafayette, IN, USA). All experiments were carried out using a conventional electrochemical cell equipped with Ag/AgCl/3 M NaCl (BAS MF-2052, RE-5B) as a reference electrode, a platinum wire (BAS MW-1032) as a counter electrode and a screen-printed graphite electrode with tyrosinase-functionalized nanoparticles as a working electrode. The screen-printing graphite working electrodes with a geometrical surface area of 0.17 cm^2 were provided by the BIOMEM Center, University of Perpignan, France and were prepared as reported previously (Andreescu et al., 2002). All the potentials were referred to the Ag/AgCl reference electrode. Distribution and size of the nanoparticles deposited onto screen-printed electrode surfaces were quantified with a JEOL JSM-7400F high resolution field emission scanning electron microscope (FE-SEM).

2.3. Procedures

2.3.1. Preparation of tyrosinase-functionalized magnetic nanoparticles (Ni and Fe_3O_4) and biosensor preparation

Enzyme functionalized magnetic nanoparticles were prepared following a previously described procedure (Rossi et al., 2004), using glutaraldehyde as a bifunctional cross-linking reagent. A colloidal nanoparticle suspension (1.7 mg mL^{-1}) was prepared by dispersing amino-functionalized magnetic particles (Ni or Fe_3O_4) in distilled water and sonicating for ∼2 h. Colloidal nanoparticles suspension was combined with glutaraldehyde (2.5% in distilled water) and tyrosinase stock solution (200 U μL^{-1} prepared in 0.1 mol L^{-1} phosphate buffer at pH 6.5) in a volume ratio 1.25:1.25:2.5 and mixed thoroughly. 5 μL of this mixture containing 100 U μL^{-1} enzyme (theoretical units) was casted onto the electrode surface and retained with a magnet, placed underneath the electrode. The enzyme modified nanoparticles-based electrode was washed with Milli-Q water to remove excess enzyme and stored at 4 °C until use. Enzyme loading and activity onto the electrode surface were estimated by performing activity tests of the immobilized enzyme by UV–Vis spectroscopy (Shimadzu UV-2401PC) using catechol as substrate. For these measurements, the working electrode containing enzyme functionalized nanoparticles was incubated in a solution of 1×10^{-4} M catechol. Activity tests were carried out by measuring the conversion of catechol to o-quinone by the immobilized tyrosinase. Appearance of quinone was measured spectrophototmetrically in the incubation solution after removing the electrode; the activity value was deduced from a calibration curve obtained with solutions of tyrosinase for which the activity was calculated using conventional protocols.

2.3.2. Preparation of the tyrosinase-functionalized gold nanoparticle biosensor

Before modification, the bare screen-printed electrode was rinsed with water and dried using a nitrogen stream. Deposition of Au nanoparticles was performed using an electrochemical procedure as described previously (Njagi et al., 2007). Briefly the electrode was immersed into 200 mg L^{-1} $HAuCl_4$ solution and a

potential of −0.20 V was applied for 1 min. The modified electrode was rinsed with water and dried under a nitrogen stream. 2.5 μL of 200 IU μL^{-1} tyrosinase was casted onto the modified electrode and allowed to dry at room temperature for 30 min before immersing it in a 2.5% (v/v) glutaraldehyde solution for 30 min. The enzyme modified electrode was washed with Milli-Q water and stored at 4 °C until use.

2.3.3. Electrochemical measurements and analytical performance measurements

Cyclic voltammetric measurements were carried out in unstirred phosphate buffer solution at pH 6.5 in the potential range from −0.4 to 0.4 V vs. Ag/AgCl, at a scan rate of 25 mV s^{-1}. Cyclic voltammetric experiments to determine the electrochemical active surface area were performed in 2×10^{-2} M potassium hexacyanoferrate (III) in 0.2 M KCl at a scan rate of 0.1 V s^{-1}. All experiments were carried out at room temperature. Amperometric measurements were performed in a 4 mL electrochemical cell containing 0.1 M PBS at pH 6.5 as supporting electrolyte. All amperometric measurements were performed at −0.15 V vs. Ag/AgCl reference electrode. The reproducibility of the biosensors was evaluated by measuring the response of at least three sensors fabricated following the same procedure. To evaluate the operational stability of the electrode, the response of the biosensor was repetitively measured by injecting the same amount of BPA substrate at a final concentration of 2×10^{-6} M and rinsing the cell between measurements.

3. Results and discussion

3.1. Cyclic voltammetric study of tyrosinase sensors based on the three types of nanoparticles

The biosensors based on the three types of materials with immobilized tyrosinase were first characterized using cyclic voltammetry to test their response to BPA, examine the effect of the nanoparticle composition on the electrochemical response, determine the electrochemical surface area and identify differences between the three configurations. Fig. 1 shows cyclic voltammograms of the bare and enzyme modified screen-printed electrodes in the presence of BPA for Au (A), Fe_3O_4 (B) and Ni (C) nanoparticles. In all cases, the enzyme tyrosinase was immobilized by cross-linking with glutaraldehyde. The electrodes with immobilized enzyme responded to BPA in both the presence and the absence of nanoparticles but with different sensitivities. The increase in the reduction peak after the addition of BPA is due to the reduction of the quinone derivative formed as a result of the enzymatic oxidation of BPA by the immobilized tyrosinase in the presence of molecular oxygen (Andreescu and Sadik, 2004; Yoshida et al., 2002). In all cases, the reduction current was proportional with the amount of BPA added.

No reduction peak for quinone was observed at the bare electrodes or at the nanoparticle-modified electrodes (Fig. 1) in the absence of enzyme. The reversible redox peak that can be seen in the background voltammogram of the bare electrode is probably due to the silver or carbon basal conducting layers of the screen-printed electrode. All three types of nanoparticles significantly increased the reduction peak of the enzymatically generated quinone as compared to that obtained with the enzyme electrode without particles. The amplified signal can be attributed to an increased conductivity of the sensor surface induced by the presence of conductive nanoparticles, and an increased surface area, providing opportunities for enhanced enzyme immobilization, substrate accessibility and enzyme–substrate interactions. The maximum reduction potential and the intensity of the current varied with the electrode material used. In all cases, a well defined

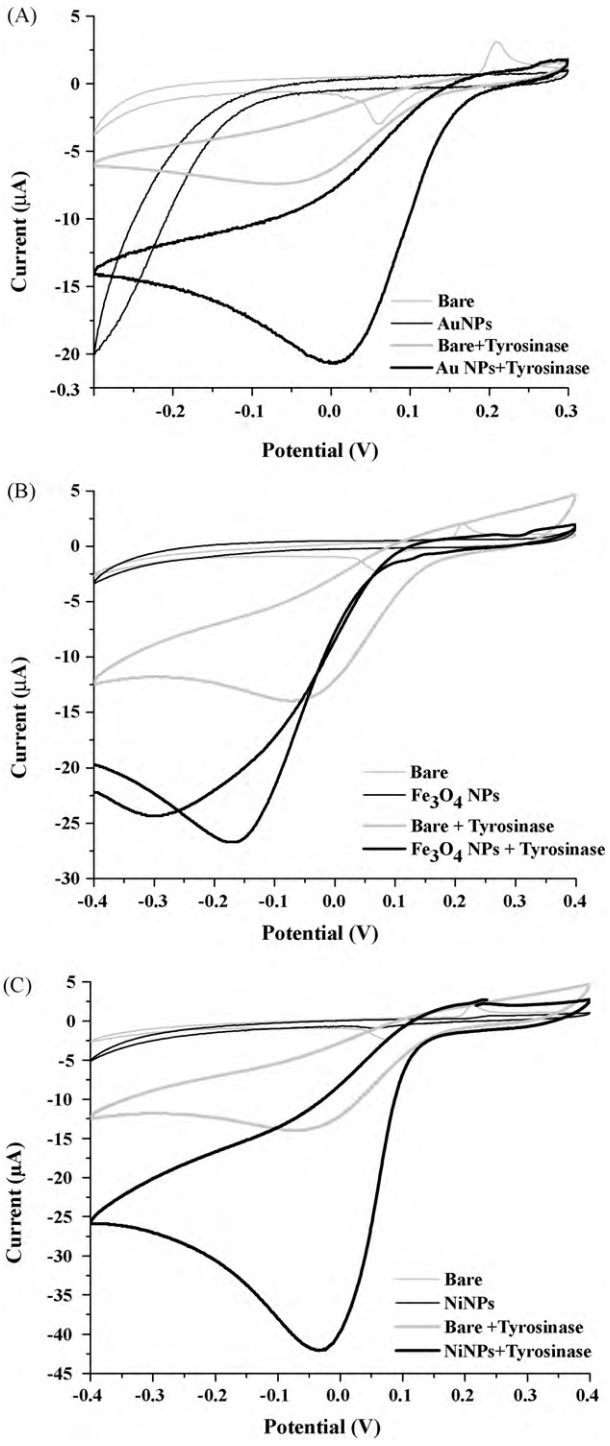

Fig. 1. Cyclic voltammograms for 2.0×10^{-4} M BPA solution at: bare electrodes, tyrosinase-modified bare electrodes Au (A), Fe_3O_4 (B) and Ni (C) nanoparticle-modified electrodes and at electrodes with tyrosinase-functionalized Au (A), Fe_3O_4 (B) and Ni (C) nanoparticles. Experimental conditions: scan rate, 25 mV s^{-1} and 0.1 M PBS at pH 6.5 as supporting electrolyte.

reduction peak in the potential range from 0.1 to −0.3 V vs. Ag/AgCl was observed, with a maximum signal-to-noise ratio at +0.02 V for Au, −0.15 V for Fe_3O_4 and −0.02 V for the Ni nanoparticles. The highest response was observed with Ni as compared to that of both Au and Fe_3O_4 nanoparticles.

To explain the recorded differences between the three configurations and the enhanced signal for the Ni nanoparticles, experiments to determine particles distribution, electrochemi-

cal surface area and enzyme loading efficiency were conducted. FE-SEM images of the nanoparticle-modified electrodes showed differences in the morphology and distribution of the particles onto the electrode surface as compared to the blank electrode (Fig. S1 in Supplementary Information). Spherical nanoparticles of Fe_3O_4 (10 nm diameter) and Ni (30 nm) covered uniformly the electrode surface, with Ni showing better polydispersity than Fe_3O_4. On the other hand, dendritic structures with aggregated 50 nm entities were observed in the FE-SEM images of electrodes with electrodeposited gold. To determine the contribution of the active area for the three nanoparticle-based electrodes, the 'real' electrochemical surface area was calculated using the Randles–Sevcik equation for a reversible process monitored by cyclic voltammetry using potassium hexacyanoferrate (III) as redox probe. The electrochemical surface area after deposition of Fe_3O_4 was nearly similar to that of the bare graphite electrode. However, significant enhancement was obtained with both Au and Ni nanoparticles, with a 5 times increase for Au, and a 1.8 times increase for Ni, as compared to the bare electrode. For Au, the enhancement can be linked to the well-organized Au nanoparticle clusters formed by electrodeposition, as seen in the FE-SEM images (Fig. S1 in Supplementary Information). These results suggest however, that the amplified BPA response obtained for Ni in the CV experiments, is not proportional and cannot be attributed solely to an enhanced surface area. Other factors such as enzyme orientation and loading efficiency onto the nanoparticle and electrode surface, release of soluble ions (e.g. soluble nickel) as well as different electrocatalytic activities of these nanoparticles towards the reduction of the enzymatically generated quinone, could be responsible for the observed biosensor response. Spectrophotometric measurements to determine enzyme loading and activity of the immobilized enzyme onto the electrode revealed loadings of 24 U per electrode of active enzyme for Fe_3O_4 vs. 64 U for the electrodes with Ni nanoparticles. This difference can contribute to the enhanced response recorded with Ni. The difference between the calculated and theoretical value of enzyme loading can be explained by a partial inactivation of the enzyme during immobilization with glutaraldehyde onto the nanoparticles as well as unfavorable orientation of the enzyme on the electrode surface after attachment of the enzyme–nanoparticle aggregates to the electrode, thus reducing the biocatalytic activity.

3.2. Analytical characteristics: sensitivity, detection limit, linear range and response time

The analytical performance of the tyrosinase biosensors was evaluated by constant potential amperometry at a potential of −0.15 V vs. Ag/AgCl. The three electrode configurations based on Au, Fe_3O_4 and Ni nanoparticles were tested in the same experimental conditions. The enzyme–magnetic nanoparticles (for Ni and Fe_3O_4) assembly was attached onto the surface of the electrode using a magnet placed underneath the electrode. For Au, the nanoparticles were electrodeposited onto the electrodes surface, resulting in a layer of high surface area Au nanoparticle clusters (Njagi et al., 2007). Fig. 2 displays typical amperometric responses for the three types of electrodes to successive additions of 2×10^{-6} M BPA to 0.1 M phosphate buffer at pH 6.5 and the corresponding calibration curves. With each addition of BPA, a well defined amperometric response proportional with BPA concentration is observed. All three biosensors responded rapidly to changes in BPA concentration, reaching 95% of the steady-state currents in less than 30 s. The response time was faster than that reported for BPA biosensors with the enzyme immobilized on carbon materials (Andreescu and Sadik, 2004; Mita et al., 2007) but longer than that reported with a chitosan–Fe_3O_4 matrix (Wang et al., 2008). The analytical characteristics of the three biosensors are summarized

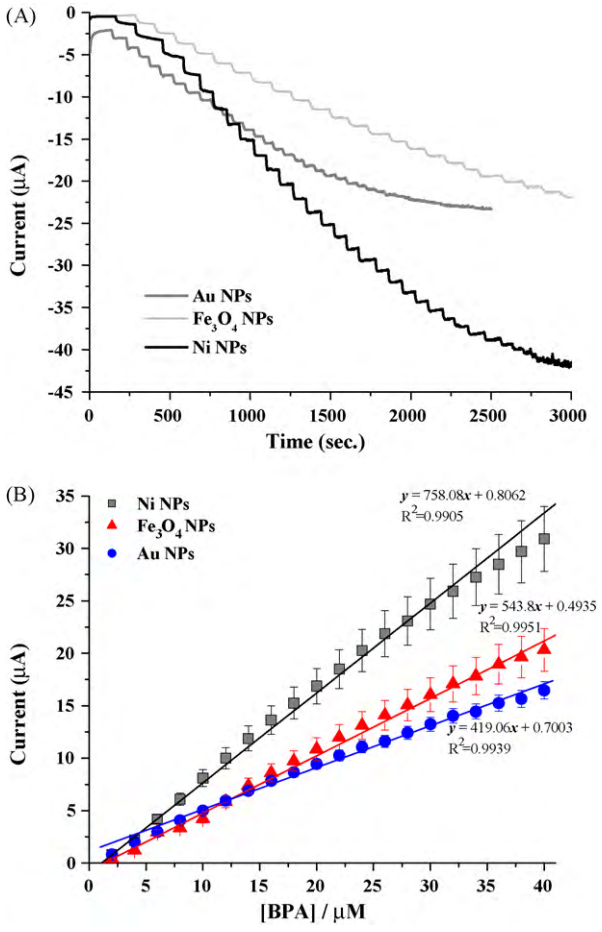

Fig. 2. (A) Typical current–time response curves for the successive additions of 2×10^{-6} M BPA in 0.1 M PBS, pH 6.5 at the tyrosinase-modified Au, Fe_3O_4 and Ni nanoparticles (NPs) based screen-printed electrodes at an applied potential of −0.15 V vs. Ag/AgCl. (B) Calibration curves for BPA obtained with the three types of biosensors (standard deviation for $n = 3$).

in Table 1, in comparison with other tyrosinase sensors reported in the literature.

Use of the nanoparticles as electrode material and enzyme immobilization matrices provided significant higher sensitivity for BPA than that reported with other biosensor configurations. The detection limits of these biosensors, calculated according to $3\sigma_s/R'$ criteria, where R' is the slope of the linear calibration curve and σ_s is the standard deviation of the amperometric signal of the blank solution were 1×10^{-8}, 8.3×10^{-9} and 7.1×10^{-9} M for Au, Fe_3O_4 and Ni nanoparticles in that order, respectively. To our knowledge, these detection limits are the lowest reported in the literature for BPA and could be attributed, as mentioned earlier, to several synergistic factors including the high surface area, enhanced conductivity and electrocatalytic activity of the different types of nanoparticles. When comparing the sensitivity of these biosensors per unit of surface, the electrodes based on Ni (10.2×10^4 μA mmol^{-1} L cm^{-2}) and Fe_3O_4 (14.2×10^4 μA mmol^{-1} L cm^{-2}) were far better than the Au-modified ones (1.96×10^4 μA mmol^{-1} L cm^{-2}). The linear range spanned over three orders of magnitude from nanomolar to high micromolar BPA concentrations for all three configurations, with at least one order of magnitude better than those reported with carbon materials (Mita et al., 2007), boron doped diamond (Notsu et al., 2002) or phenothiazine polymeric films (Dempsey et al., 2004) (Table 1).

These results demonstrate that Ni nanoparticles can be successfully used as electrode material in the construction of

Table 1
Analytical characteristics of nanoparticles-based tyrosinase biosensors for BPA and comparison with the literature data.

Biosensor configuration	E_{appl} vs. reference electrode	Analyte	Linear range (mol L^{-1})	Sensitivity ($\mu A\,mmol^{-1}\,L$)	LOD (mol L^{-1})	Response time $t_{95\%}$	References
Tyr–pTH–GCE	−200 mV vs. Ag/AgCl	Phenol	2.0×10^{-5} to 8.0×10^{-5}	44.7	1.0×10^{-6}	33 s	Dempsey et al. (2004)
		BPA	–	0.4	2.3×10^{-5}	–	
Tyr–Fe_3O_4–GCE	−200 mV vs. SCE	Catechol	8.3×10^{-8} to 7.0×10^{-5}	514	2.5×10^{-8}	–	Wang et al. (2008)
		Phenol	8.3×10^{-8} to 8.3×10^{-5}	225	2.5×10^{-8}		
Tyr–nAu–GCE	−100 mV vs. Ag/AgCl	Phenol	1.0×10^{-6} to 4.0×10^{-5}	82	2.1×10^{-7}	2 min	Sánz et al. (2005)
Tyr–APTES–BDD–GCE	−300 mV vs. Ag/AgCl	BPA	–	–	1.0×10^{-6}	–	Notsu et al. (2002)
Tyr–SWCP–CPE	−150 mV vs. Ag/AgCl	BPA	1.0×10^{-7} to 1.2×10^{-5}	138	2.0×10^{-8}	6 min	Mita et al. (2007)
Tyr–CPE	−150 mV vs. Ag/AgCl	BPA	1.0×10^{-6} to 2.0×10^{-5}	20.91	1.5×10^{-7}	3 min	Andreescu and Sadik (2004)
Tyr–AuNPs–SPCE	−150 mV vs. Ag/AgCl	BPA	4.2×10^{-8} to 3.6×10^{-5}	419.1	1.0×10^{-8}	18 s	This work
Tyr–Fe_3O_4–SPCE	−150 mV vs. Ag/AgCl	BPA	2.7×10^{-8} to 4.0×10^{-5}	543.8	8.3×10^{-9}	26 s	This work
Tyr–NiNPs–SPCE	−150 mV vs. Ag/AgCl	BPA	9.1×10^{-7} to 4.8×10^{-5}	758.1	7.1×10^{-9}	40 s	This work

pTH: poly(thionine); GCE: glassy carbon electrode; APTES: (3-aminopropyl) triethoxysilane; BDD: boron doped diamond; SWCP: single wall carbon nanotubes; AuNPs: gold nanoparticles; NiNPs: nickel nanoparticles; SPCE: screen-printed graphite carbon electrode; CPE: carbon paste electrode; SCE: saturated calomel electrode.

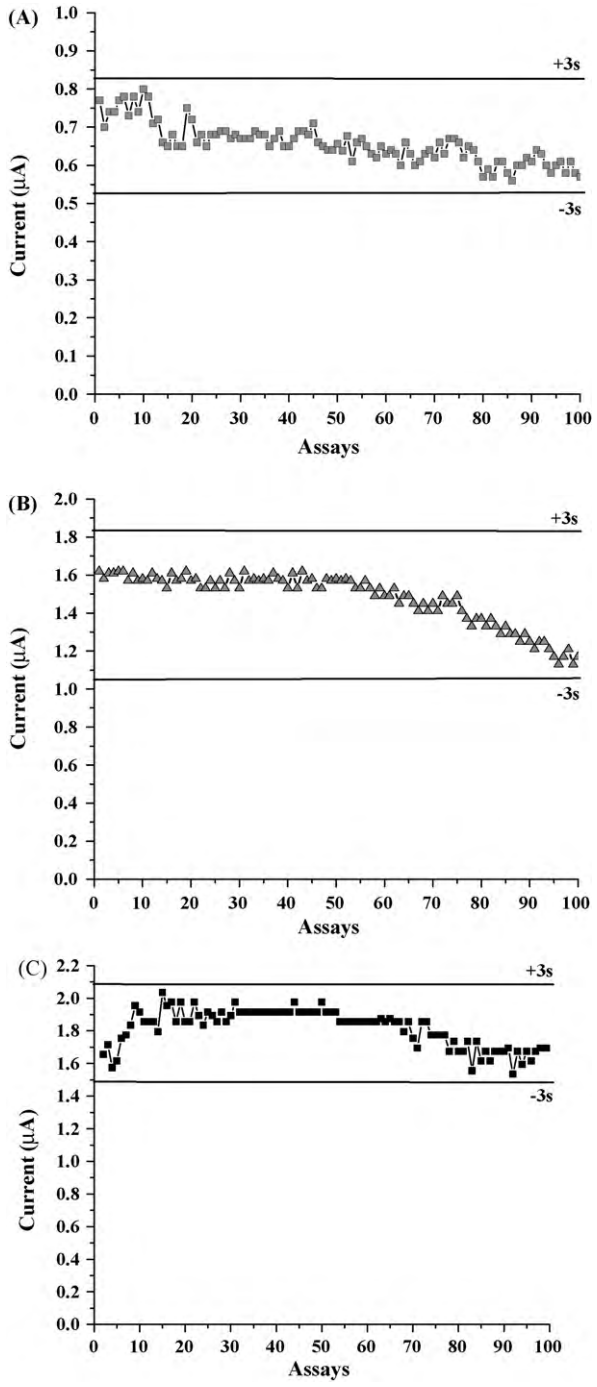

Fig. 3. Operational stability of the tyrosinase-modified Au (A), Fe_3O_4 (B) and Ni (C) nanoparticles screen-printed tyrosinase biosensors. Successive responses to the addition of 2×10^{-6} M BPA in 0.1 M PBS at pH 6.5.

electrochemical enzyme sensors for the detection of phenolic compounds. Interestingly, in spite of a lower electrochemically effective surface area, the biosensors fabricated with Ni and Fe_3O_4 demonstrated better performance than those based on Au nanoparticles, which have been widely used in the design of electrochemical enzyme biosensors. Moreover, Ni nanoparticles have magnetic properties providing capabilities for magnetic manipulation and easy handling.

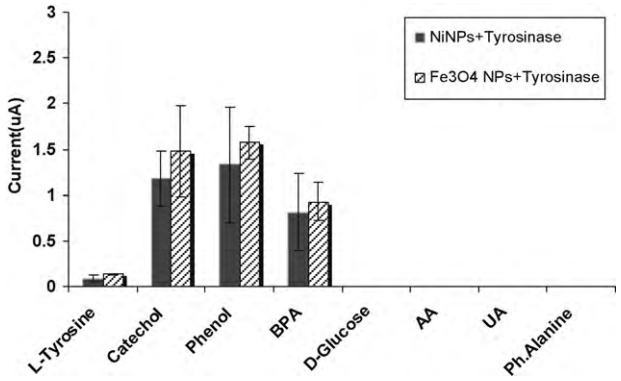

Fig. 4. Substrate specificity of the Fe_3O_4 and Ni nanoparticles screen-printed tyrosinase biosensors to the addition of 2×10^{-6} M L-tyrosine, catechol, phenol, BPA, glucose, ascorbic acid, uric acid and phenylalanine in 0.1 M PBS at pH 6.5.

3.3. Biosensor reproducibility, stability and specificity

The reproducibility of biosensors was estimated for electrodes prepared independently on different days but following the same fabrication protocol. The relative standard deviation of the sensitivity values deduced from the linear range of the calibration curves for the Au ($n = 3$), Fe_3O_4 ($n = 5$) and Ni ($n = 3$) based biosensors showed coefficients of variation of 4.7, 5.2 and 10.0%, respectively. The operational stability was evaluated by measuring the amperometric response to consecutive injections of 2×10^{-6} M BPA. Fig. 3 illustrates the operational stability of the three biosensors. The Au nanoparticle-based biosensor retained 74% of its activity after 100 assays. In the same conditions, the residual response of the Fe_3O_4 biosensor was 70% after 100 assays, while that of Ni was 98%. These results demonstrate that the biosensors can be used for multiple assays even though initially they were designed as single use disposable electrodes. This extended stability can be attributed to the covalent binding between the nanoparticles and the enzyme via glutaraldehyde, and the stable retention of the enzyme–nanoparticle assembly onto the electrode.

The specificity of the tyrosinase biosensors based on Ni and Fe_3O_4 nanoparticles was tested with several tyrosinase substrates including catechol, phenol and L-tyrosine. The electrodes responded to all three substrates but with different sensitivities (Fig. 4). Higher electrochemical responses than those obtained for BPA were recorded with catechol and phenol. This could be due to the bulkier BPA structure, inducing diffusion limitations for the biocatalytic process. On the other hand, the biosensors did not respond to common interferences like glucose, ascorbic acid, uric acid and phenylalanine, which was expected at the low operation potential of these sensors (−150 mV).

4. Conclusion

We demonstrated that Ni nanoparticles can be used as electrode material for the fabrication of electrochemical enzyme sensors for the detection of BPA. We compared the performance of these sensors with those based on the more traditionally used metal and metal oxide nanoparticles like Au and Fe_3O_4, and demonstrated that the analytical performances of the biosensors are dependent on the nanoparticle type and composition. We used these materials to immobilize tyrosinase and construct screen-printed electrodes for the ultrasensitive detection of BPA. Our results suggest that Ni provides superior characteristics in terms of sensitivity and detection limits than both Au and Fe_3O_4. All three nanoparticle-based biosensors provided very low detection limits for BPA, in the nanomolar concentration range, with the lowest limit of 7.1×10^{-9} M obtained with Ni nanoparticles. This detection limit is almost one order of magnitude lower than those reported in the literature with other types of materials and electrode designs. In addition, the Ni nanoparticles, as Fe_3O_4, have magnetic capabilities that can be useful in the design of magnetically controlled systems, flow-through columns and magneto-switchable electrochemical devices. This is the first report that compares the effectiveness of the three types of nanoparticles for electrochemical enzyme biosensors.

Acknowledgements

This work was supported by the NSF grant DMR 0804506. We thank Prof. J.L. Marty from the BIOMEM Center, University of Perpignan, France for the gift of the screen-printed electrodes and Dr. D. Goia form the Department of Chemistry and Biomolecular Science and the Center for Advanced Materials processing at Clarkson University for providing the nickel nanoparticles. RSJA acknowledges financial support from the Iraqi Government who supported his research stage in the US.

Appendix A. Supplementary data

Supplementary data associated with this article can be found, in the online version, at doi:10.1016/j.bios.2010.05.001.

References

Andreescu, S., Barthelmebs, L., Marty, J.L., 2002. Analytica Chimica Acta 464 (2), 171–180.
Andreescu, S., Sadik, O.A., 2004. Analytical Chemistry 76 (3), 552–560.
Avramescu, A., Andreescu, S., Noguer, T., Bala, C., Andreescu, D., Marty, J.L., 2002. Analytical and Bioanalytical Chemistry 374 (1), 25–32.
Ballesteros-Gomez, A., Rubio, S., Perez-Bendito, D., 2009. Journal of Chromatography A 1216 (3), 449–469.
Chang, C.M., Chou, C.C., Lee, M.R., 2005. Analytica Chimica Acta 539 (1–2), 41–47.
Chen, D.H., Liao, M.H., 2002. Journal of Molecular Catalysis B: Enzymatic 16 (5–6), 283–291.
Chen, X., Cheng, G.J., Dong, S.J., 2001. Analyst 126 (10), 1728–1732.
Dekant, W., Voelkel, W., 2008. Toxicology and Applied Pharmacology 228 (1), 114–134.
Dempsey, E., Diamond, D., Collier, A., 2004. Biosensors & Bioelectronics 20 (2), 367–377.
Fievet, F.L.J.P., Figlarz, M., 1989. MRS Bulletin, 29–34.
Huang, S.-H., Liao, M.H., Chen, D.H., 2003. Biotechnology Progress 19, 1095–1100.
Ispas, C., Andreescu, D., Patel, A., Goia, D., Andreescu, S., Wallace, K., 2009. Environmental Science and Technology 43 (16), 6349–6356.
Istarnboulie, G., Andreescu, S., Marty, J.L., Noguer, T., 2007. Biosensors & Bioelectronics 23 (4), 506–512.
Kang, J.-H., Kondo, F., Katayama, Y., 2006. Toxicology 226 (2–3), 79–89.
Katz, E., Willner, I., 2002. Journal of the American Chemical Society 124 (35), 10290–10291.
Le, H.H., Carlson, E.M., Chua, J.P., Belcher, S.M., 2008. Toxicology Letters 176 (2), 149–156.
Li, Y.F., Liu, Z.M., Liu, Y.L., Yang, Y.H., Shen, G.L., Yu, R.Q., 2006. Analytical Biochemistry 349 (1), 33–40.
Liu, S.Q., Yu, J.H., Ju, H.X., 2003. Journal of Electroanalytical Chemistry 540, 61–67.
Liu, Z.M., Liu, Y.L., Yang, H.F., Yang, Y., Shen, G.L., Yu, R.Q., 2005. Analytica Chimica Acta 533 (1), 3–9.
Loaiza, O.A., Laocharoensuk, R., Burdick, J., Rodriguez, M.C., Pingarron, J.M., Pedrero, M., Wang, J., 2007. Angewandte Chemie International Edition 46 (9), 1508–1511.
Lu, B.W., Chen, W.C., 2006. Journal of Magnetism and Magnetic Materials 304 (1), E400–E402.
Lu, L.M., Zhang, L., Qu, F.L., Lu, H.X., Zhang, X.B., Wu, Z.S., Huan, S.Y., Wang, Q.A., Shen, G.L., Yu, R.Q., 2009. Biosensors & Bioelectronics 25 (1), 218–223.
Mena, M.L., Yanez-Sedeno, P., Pingarron, J.M., 2005. Analytical Biochemistry 336 (1), 20–27.
Mita, D.G., Attanasio, A., Arduini, F., Diano, N., Grano, V., Bencivenga, U., Rossi, S., Amine, A., Moscone, D., 2007. Biosensors & Bioelectronics 23 (1), 60–65.
Nerin, C., Philo, M.R., Salafranca, J., Castle, L., 2002. Journal of Chromatography A 963 (1–2), 375–380.
Njagi, J., Andreescu, S., 2007. Biosensors & Bioelectronics 23 (2), 168–175.
Njagi, J., Warner, J., Andreescu, S., 2007. Journal of Chemical Education 84 (7), 1180–1182.
Nomura, A., Shin, S., Mehdi, O.O., Kauffmann, J.M., 2004. Analytical Chemistry 76 (18), 5498–5502.

Notsu, H., Tatsuma, T., Fujishima, A., 2002. Journal of Electroanalytical Chemistry 523 (1–2), 86–92.
Park, H.Y., Schadt, M.J., Wang, L., Lim, I.I.S., Njoki, P.N., Kim, S.H., Jang, M.Y., Luo, J., Zhong, C.J., 2007. Langmuir 23 (17), 9050–9056.
Rossi, L.M., Quach, A.D., Rosenzweig, Z., 2004. Analytical and Bioanalytical Chemistry 380 (4), 606–613.
Salimi, A., Sharifi, E., Noorbakhsh, A., Soltanian, S., 2006. Electrochemistry Communications 8 (9), 1499–1508.
Salimi, A., Sharifi, E., Noorbakhsh, A., Soltanian, S., 2007. Biosensors & Bioelectronics 22 (12), 3146–3153.
Sanz, V.C., Mena, M.L., Gonzalez-Cortes, A., Yanez-Sedeno, P., Pingarron, J.M., 2005. Analytica Chimica Acta 528 (1), 1–8.
Stanciu, L., Won, Y.H., Ganesana, M., Andreescu, S., 2009. Sensors 9 (4), 2976–2999.
Tu, X.M., Yan, L.S., Luo, X.B., Luo, S.L., Xie, Q.J., 2009. Electroanalysis 21 (22), 2491–2494.
Volkel, W., Kiranoglu, M., Fromme, H., 2008. Toxicology Letters 179 (3), 155–162.
Wang, J., Musameh, M., Laocharoensuk, R., 2005. Electrochemistry Communications 7 (7), 652–656.
Wang, J., Scampicchio, M., Laocharoensuk, R., Valentini, F., Gonzalez-Garcia, O., Burdick, J., 2006. Journal of the American Chemical Society 128 (14), 4562–4563.
Wang, S.F., Tan, Y.M., Zhao, D.M., Liu, G.D., 2008. Biosensors & Bioelectronics 23 (12), 1781–1787.
Won, Y.H., Jang, H.S., Kim, S.M., Stach, E., Ganesana, M., Andreescu, S., Stanciu, L.A., 2010. Langmuir 26 (6), 4320–4326.
Yoshida, M., Ono, H., Mori, Y., Chuda, Y., Mori, M., 2002. Journal of Agricultural and Food Chemistry 50 (15), 4377–4381.